Article

Cellular Automata Based Land-Use Change Simulation Considering Spatio-Temporal Influence Heterogeneity of Light Rail Transit Construction: A Case in Nanjing, China

Jiaming Na [1], **Jie Zhu [2],***, **Jiazhu Zheng [2]**, **Shaoning Di [2]**, **Hu Ding [3]** and **Lingfei Ma [4]**

1   Key Laboratory of Virtual Geographic Environment (Nanjing Normal University), Ministry of Education, Nanjing 210023, China; jiaming.na@njnu.edu.cn
2   College of Civil Engineering, Nanjing Forestry University, Nanjing 210037, China; zjz90139@njfu.edu.cn (J.Z.); dsn17@njfu.edu.cn (S.D.)
3   School of Geography, South China Normal University, Guangzhou 510631, China; hu_ding@m.scnu.edu.cn
4   Beijing Transportation Information Center (BTIC), Beijing 100073, China; malingfei@jtw.beijing.gov.cn
*   Correspondence: chu_je@njfu.edu.cn

Abstract: Light rail transit (LRT), an essential urban public transport system in China, significantly reshaped the urban land-use (LU) pattern. Although the LRT impact and land-use change (LUC) analysis plays an essential role in urban planning policy, the spatiotemporal heterogeneity of LRT impacts have not been considered in LUC simulation studies. This study simulates the urban LU change, considering the spatiotemporal heterogeneity of LRT construction impacts on urban LUC. LUC from 1995 to 2005 in Nanjing, China, is chosen as a case study. At first, the distance decay function is employed to verify the quantitative impact of LRT construction on LU change. Accordingly, the variation trends of each LU type during different stages are described in time and space. A cellular automata model incorporated by the generated LRT impact is established and then implemented for simulation. According to model performance assessment results, the proposed model can produce a realistic urban pattern with Freedom of Movement (FoM) exceeding 24% and a significantly lower relative error than the CA simulation without considering LRT influence.

Keywords: light rail transit (LRT); spatiotemporal heterogeneity; land-use change; cellular automata (CA)

1. Introduction

Land-use change (LUC) has been widely studied in the past few decades [1–4]. This topic deals with the sustainable development of natural and anthropogenic systems and their influences on air, water, soil, and human habitat. According to the performed studies, the LUC dynamics variations lead to irreversible impacts of human activities on the environment [4]. These variations lead to a complex process driven by a series of natural and social factors [5–7]. Furthermore, the conversion and modification of the LUC caused by human activities and natural processes may cause various environmental and ecological problems. Accordingly, LUC tightly relates to various important socioeconomic and environmental issues [8–10]. Thus, a detailed understanding of urban dynamics is essential in regional and global sustainable development.

According to the Sixth National Population Census of the People's Republic of China, China's urban population growth has peaked from 36.22% to 49.68% from 2000 to 2010 [11]. As a result, sharp population growth and rapid land development of some megalopolis (e.g., Shanghai, Wuhan, Nanjing) led to traffic congestion and the deterioration of living environments [12,13]. Constructing urban light rail transit (LRT) is a high priority for Chinese governments to overcome these problems [14,15]. In China, LRT has become the mainstream for the urban public transport system due to its advantages, including high efficiency, large capacity, small above-ground space occupation, and less pollution [16,17].

The LRT development provides a foundation for optimizing urban space layout and a great opportunity to reconstruct urban land-use patterns [18–20].

The analysis of the relationship between LRT and LUC plays an essential role in the urban planning and development/management policy [21,22]. Since 1960, the interactions between LRT and land-use development have been well recognized. A new rail transit line construction leads to transportation accessibility improvement and developable land resource growth, indicating a positive and noticeable impact on both urban development (e.g., labor market, crime rate, and public discourse) and property values surrounding service areas [20,23–25]. Some studies have demonstrated that LRT profoundly impacts urban land-use development by effectively creating higher intensity and more compact development that occurred near rail stations based on the land-use data [26,27]. Others concluded that the rapid transit system could only influence land cover change in peripheral areas, but not increase the developed center area along rail lines and stations [28]. However, as pointed out in some studies, since the LRT construction usually occupies several land resources, the rail transit may harm land-use (LU) development [19,27,29,30]. As a consequence, the LRT can damage the ecological environment and threaten human health. Moreover, various studies have been devoted to urban rail traffic spatiotemporal effects on LU [20,31–33]. The impact of rail transport on LU can vary at different stages, including design, planning, construction, and operation [31,34]. It can also vary depending on the urban areas and LU types. Various quantitative methods have considered the impacts of transit on land-use development, such as index comparisons [22], regression models [35], and statistical significance tests [36]. However, although the existing literature mainly focuses on the impacts of LRT on previous LU development, it is noticeable that it does not analyze their effect on the future spatial growth, which is crucial to regional planning.

The simulation and prediction of the potential changes of urban LU according to the LRTs' development have been recently performed. Some models, such as UrbanSim [18] and Cellular Automata (CA) [21,37–40], have been proposed to investigate the influence of LRT in the LUC simulation. Previous LUC simulation shows that the CA model performs well in LUC simulation, although it is always challenging. CA is frequently utilized to simulate historical growth and model the dynamic urban development, which provides greater simplicity and a more precise representation of the dynamics of the LU change [41,42]. In this model, the transition rules are described with a location choice optimization problem that maximizes land suitability with the impact of some selected driving factors. Introducing the influence of LRT into the simulation helps us to understand the urban LUC process better. The common studies have addressed the interaction between urban LU change and LRT stations. LRT can encourage high-density, mixed-use land development near the stations, leading to more fragmented land patterns near LRT stations than the other areas. For example, different extents of impacts of rail transit stations (e.g., 10 min walking distance, half-mile catchments) on LU changes have been proposed to address the relationship between transportation networks and LU patterns and simulate land development around station using the CA model [38,43]. A multinomial logistic regression (LR) approach is commonly utilized to quantify the linear or nonlinear relationship between driving factors and LU change. These results indicate how rail transit stations shape the fine-scale LU change information in the small-scale region [39,40]. However, few efforts focus on the interaction between urban LU change and LRT lines in time and space. Although previous works have considered the influence of LRT on LUC, most studies derived empirical results on LRT's impact on urban LU development. It has been reported that the LRT construction could induce an inhomogeneous spatial impact on urban LU under time-varying spatial impacts [38,40]. Although LRT has been studied as an essential driving factor in LUC modelling, few studies have investigated the heterogeneous external interference of LRT on LU development in temporal and spatial dimensions. On the other hand, the LRT influences on LUC have indicated a changed tendency with the LRT distance in space [44–46]. This spatial heterogeneity of distance variations from LU blocks to LRT

also has rarely been considered for LUC simulation studies. The temporal difference of LRT influence has not been considered in the literature. Generally, the life cycle of LRT consists of four stages: planning, construction, operation, and management [31,34]. Since the spatial effect of LRT on their surrounding LU is of no doubt dynamic in different stages, an LUC model considering the spatiotemporal heterogeneity of LRT influence should be established for accurate simulation of the LUC process.

This study attempts to simulate the urban LUC considering the spatiotemporal heterogeneity of LRT influence, based on the above motivations. Since it is only focused on the influence of LRT construction, the historical urban development during LRT construction is considered. The LUC of Nanjing, China, from 1995 to 2005, the construction period of Nanjing LRT Line 1, is selected as a study case. At first, the distance decay function method is employed to evaluate the impact of LRT on LUC quantitatively. According to the LU change direction and the distance to LRT, this function provides an attraction or repulsion value. Then, the discrepancy trends of each LU type are explained in time and space for different years. Finally, the generated relationship between LRT construction and LUC is employed to establish a cellular automata (CA) model incorporated by LRT influence and implement it for LUC simulation.

2. Study Area and Materials

The city of Nanjing (Jiangsu Province, China) is selected as a study case due to its rapid urbanization and population increase [47]. As shown in Figure 1, Nanjing is one of the most important gateway cities of China, located in the Yangtze River Delta, which comprises of seven districts with a total area of 6597 km^2. Although previous LUC models have been reported in the literature [48,49], a spatiotemporal heterogeneous CA model is established in this study. The construction of Nanjing LRT Line 1 begun in 2000 and went into operation on 3 September 2005. It passes through the Jiangning, Downtown (Zhucheng), and Qixia Districts. Therefore, the simulation results of these three districts will be emphasized in this study.
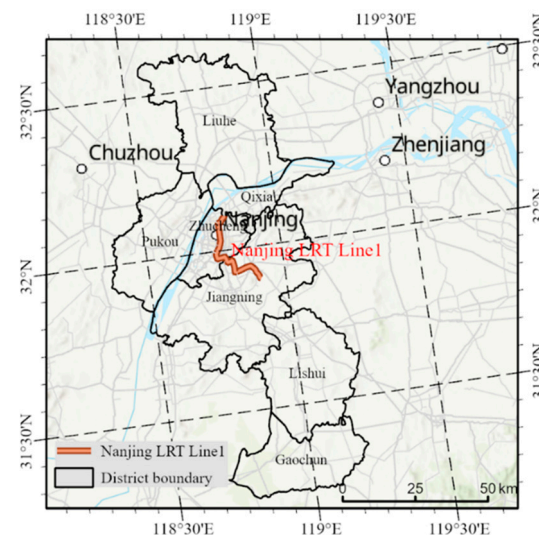
Figure 1. The city of Nanjing and Nanjing LRT Line 1.

As shown in Figure 2, the urban LU data with 30 m spatial resolution in 1995, 2000, and 2005 are utilized in this study. This dataset was published by the Geographical Information Monitoring Cloud Platform (Available online: http://www.dsac.cn/, accessed on 3 March 2021), generated by manual interpretation from Landsat TM/ETM+/OLI image. The LU data includes six LU types: farmland, forest, meadow, water, construction, and unused. The overall classification accuracy of the farmland and construction is higher than 85%, while it is higher than 75% for the other LU types.

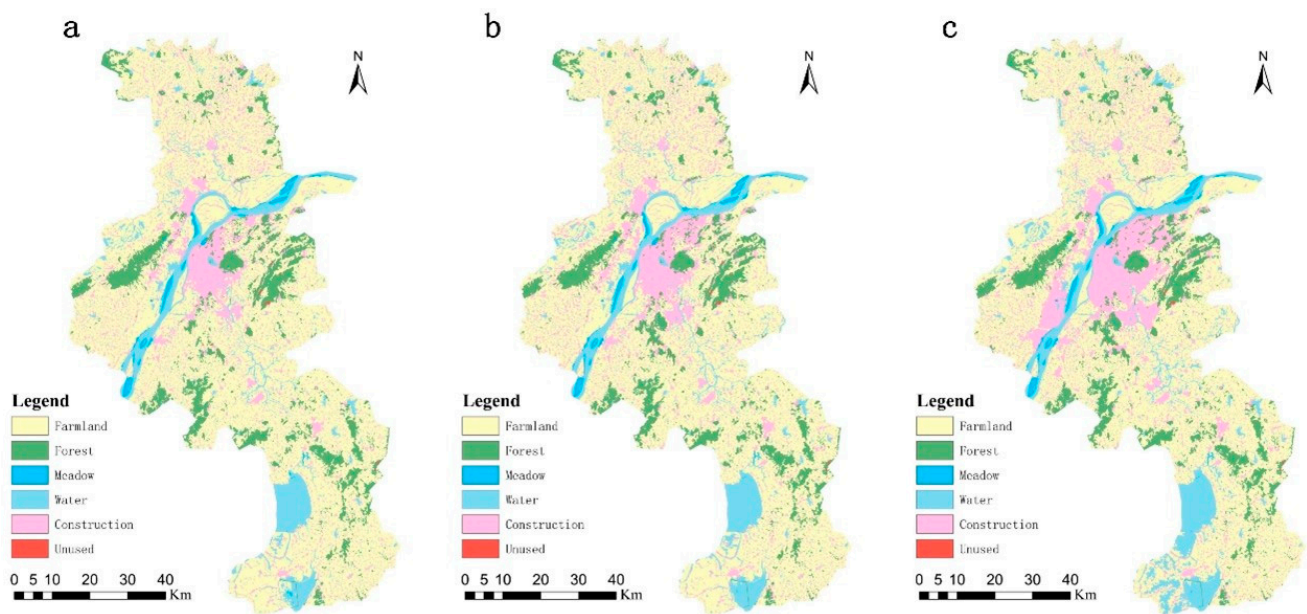**Figure 2.** LU data in the years of (**a**) 1995, (**b**) 2000, and (**c**) 2005.

The road network, digital elevation model (DEM), and the master plan of Nanjing city are also employed to analyze and model the LUC's driving factors. The road network published by National Earth System Science Data Center contains different roads, including railway, national highway, highway, and county and town roads. This dataset is adopted to analyze the relationship between the distance to different level roads and LUC. The master plan of Nanjing city (1991–2010), officially published by the Nanjing Urban Planning Administration Bureau, can generate different-level city/county centers, farmland protection, and habitat conservation areas for further analysis. SRTM DEM is utilized to calculate the slope and verify its impacts on LUC.

3. Methodology

3.1. Basic Ideas of the Proposed CA Model

As a spatially explicit modelling method, CA simulates complex systems using local cell interactions and global drivers. Traditional CA components include cell state, neighborhood influence, urban transition potential, and fixed constraints [50]. Cell state changes are defined based on transition rules that reflect the combined interactions of these components. The primary structure of the transition rules is specified as:

$$P_{total} = P(S_i^{t+1} | S_i^t, N, T, Con) \tag{1}$$

where P_{total} is the total transition potential; S_i^t and S_i^{t+1} are the states of the cell i at time t and t + 1, respectively; N describes the influence of cell's neighborhood; P is the transition potential defined by several drivers; Con includes the effect of any spatial and nonspatial constraints.

In this study, a square 5×5 neighborhood window was selected, details of this will be discussed in Section 3.3.1. The urban transition potential T and transition constraint Con are defined using 4 selected drivers (topographic, planning, urban development, and LRT construction). Table 1 shows the spatial variables employed to construct the CA model. The topographic variable is mainly calculated by the slope derived from DEM. The distance variables are defined as the Euclidian distances to each entity, computed by the Euclidean distance function of ArcGIS software. Planning restriction is generally extracted directly from the master plan map. The LRT factor, a decay function fitting between distance to LRT line and LUC, was conducted. The detailed design of the CA model will be introduced in

the following section. Compared to classic CA models, the LRT impact was adopted as a spatial constraint to reflect spatial heterogeneity in urban development.

Table 1. Spatial variables applied to build the CA model.

	Spatial Variables	Data Source	Calculation Method
Topographic constraint	Slope	DEM	Slope tool in ArcGIS
Planning Restriction constraint	Farmland protection Habitat Conservation	Master plan	Extract and reclassify
Distance Factor	Distance to water (d_1) Distance to railway (d_2) Distance to highway (d_3) Distance to national highway (d_4) Distance to provincial road (d_5) Distance to county road (d_6) Distance to municipal center (d_7) Distance to county center (d_8)	LU Road network Master plan	Euclidean distance function
LRT Construction Factor	LRT	Road network	Euclidean distance function and Gauss decay function

Figure 3 illustrates our workflow for examining the spatial-temporal heterogeneity of LRT influence on urban LUC simulation. At first, 1995, 2000, and 2005 urban land patterns were generated from the LU data, and the LRT line was extracted from road network data. A small set of urban development driving factors were generated to train the CA model. The CA transition rules were constructed based on samples selected from historical (1995–2000) urban patterns and their drivers. The CA model was then constructed by integrating the four drivers, and the LU was implemented in 2005.

3.2. Transition Potential (T) and Constraint (Con) Establishment

As mentioned above, the next state of the target cell in the CA model is estimated based on the current state and its neighboring cells by using transition rules. The driving factors could model the transition rules. In this study, 4 driving factors were selected, including topographic, planning, urban development, and LRT construction.

3.2.1. Topographic Constraint (Con_{topo})

The local topography can control the LUC process. For example, the land is no longer suitable for farming when its slope degree exceeds 15°. Thus, the topographic factor is utilized to restrict the LU type transition based on the slope degree calculated from DEM. It was designed as follows:

$$Con_{topo} = \begin{cases} Con_{S_i \to construction} \left(slope \leq 25^{\circ}\right) \\ Con_{S_i \to farmland} \left(slope \leq 15^{\circ}\right) \\ Con_{S_i \to water} \left(slope \leq 2^{\circ}\right) \\ Con_{S_i \to forest} \left(slope > 6^{\circ}\right) \\ Con_{S_i \to unused} \left(slope > 6^{\circ}\right) \end{cases} \quad (2)$$

where Con_{topo} is the topographic constraint that returns 1 for a suitable cell for the LU transition. Note that meadowland does not have a proper condition due to its low sensitivity to the slope degree.
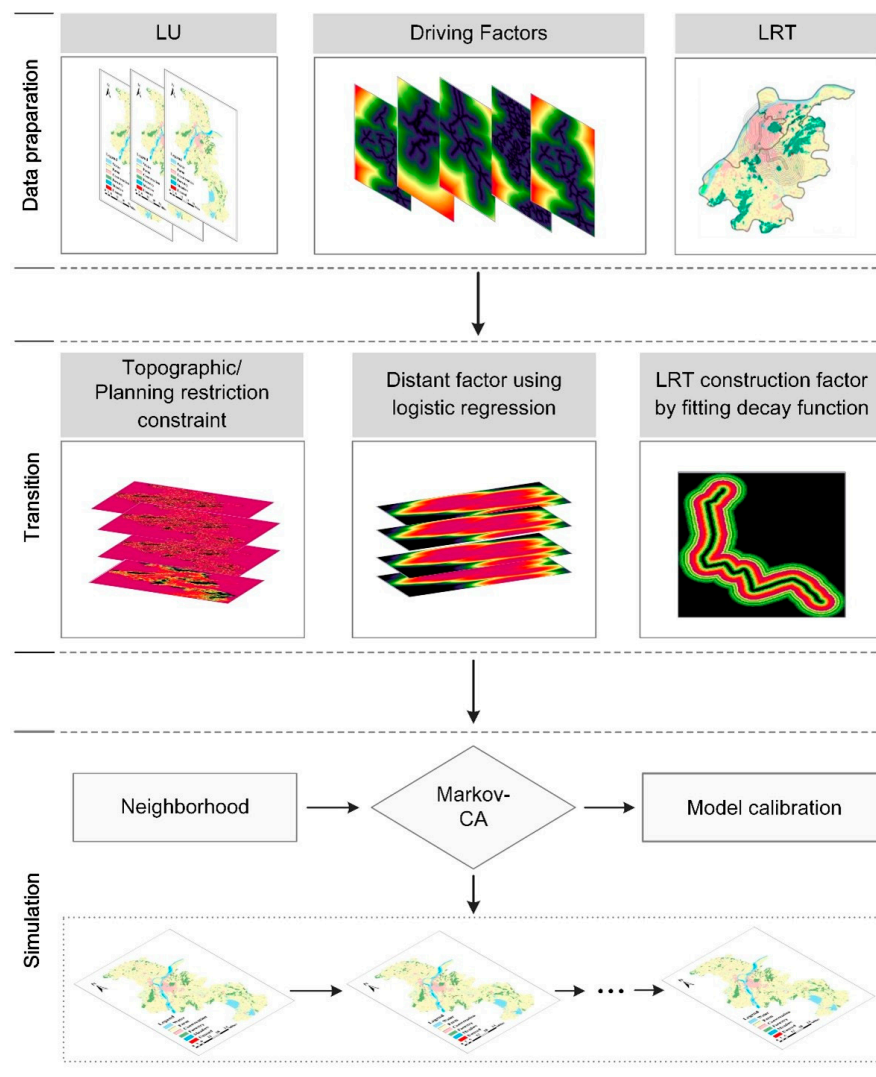
Figure 3. Workflow for evaluation of the spatiotemporal heterogeneity impact of LRT on LU change.

3.2.2. Planning Restriction Constraint ($Con_{planning}$)

The LUC process can also be controlled by urban planning. In China, the master plan published by the local government defines the restriction of specific areas for the LU-type transition. The planning restriction factor can be defined based on the Master Plan data as:

$$Con_{planning} = \begin{cases} If\ S_i^t \in (farmland\ protection, habitat\ conservation) \\ then\ S_i^{t+1} = U,\ U \in (farmland, forest, meadow); \\ If\ S_i^t \in (construction\ planning\ area) \\ then\ S_i^{t+1} = U, U \in (construction); \\ If\ S_i^t \in (No\ building\ planned\ area) \\ then\ S_i^{t+1} = U,\ U \in (unused) \end{cases} \tag{3}$$

where $Con_{planning}$ is the planning constraint; U stands for the LUC restriction in the master planning. For example, if the cell S_i is located in habitat conservation and farmland protection areas in the master planning, the conversion of cell S_i will be restricted to forest, meadow, and farmland.

3.2.3. Distance Factor ($P_{distance}$)

The spatial distances to certain geographic features (e.g., water, road, city center, etc.) will also influence the LUC process. Logistic regression (LR) is commonly adopted

to determine different spatial distance variables' weights for the recursive calculation of the transition probability [5]. Distances to water, railway, highway, national highway, provincial road, county road, municipal center, and county center were considered. A stratified random sampling method is employed to extract 20% of samples from the distance variables and discover the CA model's transition rules. The LR model statistically determines the suitability of each cell, where multiple variables are weighted combined:

$$P_{distance} = \frac{1}{1 + exp\left(-(\beta_0 + \sum_{i=1}^{8} \beta_i \times d_i)\right)}, \tag{4}$$

where $P_{distance}$ measures the LU transition suitability based on the LR model; $[d_1, d_2, \ldots, d_8]$ are the distance variables to water, railway, highway, national highway, provincial road, county road, municipal center, and county center, respectively; $[\beta_0, \beta_1, \ldots, \beta_8]$ are the regression coefficients for the different variables.

3.2.4. LRT Construction Factor (P_{LRT})

According to previous studies, transportation facilities' construction can make the urban land spatially inhomogeneous, while the spatial impact continuously varies dynamically over time. The traditional ring-based analysis is firmly grounded in classic urban theory, which assumes a homogeneous spatial effect. This bias limits its capability when analyzing the LRT influence on LUC. Some studies focused on half-mile (804.7 m) catchments of station areas, corresponding to around 10 min walking distance [51,52] to investigate the relationship between urbanization and LU. Kwoka et al. (2015) [53] pointed out that a 15-min walk (approximately 1200 m) shed to stations would provide a more realistic analysis. Some previous works [21,39,40,54] constructed a two-sided multi-ring buffer to evaluate the impacts of LRT on surrounding urban land-use. In the existing body of literature on the interactions between LU and LRT, Euclidean distance has been commonly utilized to determine the spatial extent of LRT and analyze the gradual transition of LU changes within different ranges. Therefore, a standard method is employed for defining the spatial influence extent of the LRT line based on concentric ring partitioning. The year-by-year LU change maps from 1995 to 2000 are firstly created to evaluate the LRT impacts on its neighboring urban LU change. The relative change rate K_{ij} through buffer operations is then calculated to reflect the LRT spatiotemporal heterogeneity influence as:

$$K_{ij} = \frac{A_{ij}}{A_j} \times 100\% \tag{5}$$

where A_{ij} represents the transfer area of i_{th} LU (the construction farm area in this study) within the j_{th} buffer zone, A_j is the total LU changed area within the j_{th} buffer zone.

Pre-analysis (see details in Section 4.1.2) indicates a clear distance decay trend between K_{ij} and distance (d) to LRT. This trend can then be fitted by the decay function K(d) using MATLAB 2014(a) software. The fitted decay function can quantitatively describe the rule of urban LU change distribution near or away from the LRT and provide the spatial information for urban dynamics simulation. Finally, the LRT factor can be defined by the following equation:

$$P_{LRT} = normalized\left(K(d) \times \frac{t - t_0}{T}\right) \tag{6}$$

where the output P_{LRT} describes the LRT factor, which is normalized to the range of [0, 1]; T denotes the period length (measured in years in this case); d depicts the distance to LRT line; and t_0 and t describe the initial and mid-term construction years, respectively.

3.2.5. Final Transition Probability

The aforementioned 4 different factors should be then combined to determine each cell's transition probability. To attain this goal, the final transition probability is computed as follow:

$$P^t_{total} = Con_{topo} \times Con_{planning} \times P_{distance} \times P_{LRT} \tag{7}$$

where P^t_{total} describes the overall cell's land-use change possibility. The cell should meet the global urban development and neighborhood constraints while its LU state accordingly changes.

3.3. Other Model Parameter Setting

3.3.1. Neighborhood (N)

In this study, an extended Moore neighborhood configuration (5×5) was employed in which each cell indicates an area of 30 m $\times$ 30 m on the ground for the simulation [55]. In the neighborhood, LU types of the other cells, except the target cell, were first recorded. The greater the number of specific LU types in the neighborhood, the greater the probability that the target cell will be converted into this LU type.

3.3.2. Transition Possibility Threshold ($P_{threshold}$)

The transition probability $P_{threshold}$ should be determined before running the CA model. Taking the reference map of 1995 as a basis, the LU changes in 2000 were simulated by computing the transition probability P of each cell by neglecting the LRT impact. For the computed transition probability P of a cell, if $P > P_{threshold}$, the LU type will be changed. Some LU samples were randomly selected to estimate the range of $P_{threshold}$ through a recursive procedure during the simulation. The optimal $P_{threshold}$ was determined by analyzing the CA modeling performance. The Freedom of Movement (FoM) indicator (see details in Section 3.4) was chosen to assess the model's performance, where $P_{threshold}$ could be determined when the FoM achieves the best.

3.3.3. Iteration Ending Condition

The CA model can model the dynamics of LU change over several iterations, where every LU type will typically lose some of its lands to one or more of the other classes (and it may also gain land from others). A Markov chain analysis could be employed to extract the quantities and percentages of conversion between each LU type from the historical LUC (i.e., from 1995 to 2000). The transition area matrix is utilized as the guideline for the quantitative transformation in simulating the LU change. The constrained control was adopted to determine the iteration number for providing the construction land area that reaches the total transformation value.

3.4. Model Performance Assessment

The FoM indicator proposed by Pontius et al. (2008) could be adopted to evaluate the simulation accuracy by comparing different and common areas between simulation results and the actual map [6]. The FoM is defined as follows:

$$\text{FoM} = \frac{B}{A + B + C + D} \tag{8}$$

where A represents the area changing, while it does not change during the simulations, B is the common area changing in both the actual map and simulations. C denotes the area changing in both the actual and simulated maps, while the LU change types are different. D is the area that does not change in the actual map, while it changes during simulations. Typically, satisfactory simulation results can be obtained when the FoM is up to 0.21.

4. Results and Discussions

4.1. CA Transition Rule Result

As already mentioned, four driving factors, including topographic constraint, planning restriction constraint, distance factor, and LRT factor, were utilized to construct the transition probability of each cell. Accordingly, the CA models were calibrated and validated. The topographic and planning restriction constraints could be easily generated by raster reclassifying from the slope calculation and master plan.

4.1.1. Distance Factor

Seven spatial distance driving factors (see detail in Section 3.2.3) were utilized to evaluate the LUC potential. LR was applied to determine spatial variables' weights. Table 2 presents the estimated coefficients and their corresponding statistics. The stepwise forward eliminates the redundant variables in LR, such as distances to a national highway and a municipal center. Table 2 shows the estimated coefficients for the spatial variables.

Table 2. The coefficient of binary logistic regression for each LU type.

Coefficient/LU	Farmland	Forest	Meadow	Water	Construction
β_1	0.63	0.33	−1.35	-	0.65
β_2	−0.20	−0.36	3.55	−0.12	-
β_3	−2.40	-	2.25	2.43	1.25
β_5	1.50	−1.82	−1.96	−1.52	−0.72
β_6	-	−1.05	1.56	0.67	0.85
β_7	−1.52	−0.86	2.52	3.23	−1.85
β_0	0.55	0.55	−5.35	−0.23	−0.45

Notes: The unused LU type is excluded since its change is irregular with spatial distance factors.

4.1.2. LRT Factor

A series of 0.2-km buffers were created step-by-step from the LRT line to assess its impacts on the surrounding urban LU. Although previous case studies in Chinese cities demonstrated that a 1~2 km buffer could quantify the LRT influences on LU [38,39], these works were mainly focused on the development of detailed urban LU such as industrial/commercial lands. Yang et al. (2019) has employed a 3.2 km buffer associated with rail transit line to investigate the spatial effects of subways on the construction LU changes [40]. These studies are employed in this work to construct a 3.2 km two-sided, multi-ring buffer at the interval of 0.2 km for LRT in Nanjing to evaluate its influences on neighboring urban LU, considering LU type information and barrier effect (e.g., Yangzi River in Figure 2).

Figure 4 depicts the variation maps of different LU types associated with rail transit lines from 2000 to 2005. There are two LU change directions, including construction to farmland and farmland to construction. Statistical results show that the LUC direction farmland to construction occurs more than 95% of all of the LUC directions, which can be considered the chief contributor in each buffer ring. Thus, the change in direction of farm to construction is utilized to evaluate the LRT impacts.

Figure 5 shows the relative change rate K_{ij} between the years 1995 and 2000. LRT's spatial effect on construction land can be described as: (1) The LRT has considerable effects on construction land development, while the total amount of construction land around the line significantly increases. (2) According to a nonlinear relation, moving away from the LRT line leads to an irregular decline in the growth rate of construction LU change.
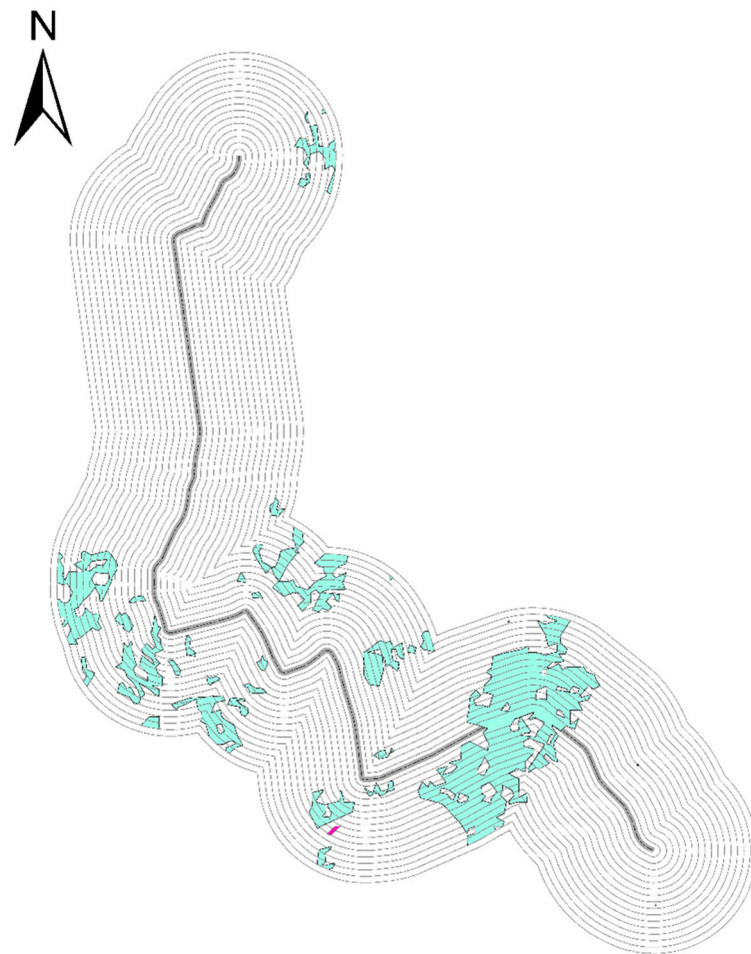
Figure 4. LUC maps associated with the LRT line from 1995 to 2000. Different rings show the buffer zone from the LRT with a 0.2 km zone.
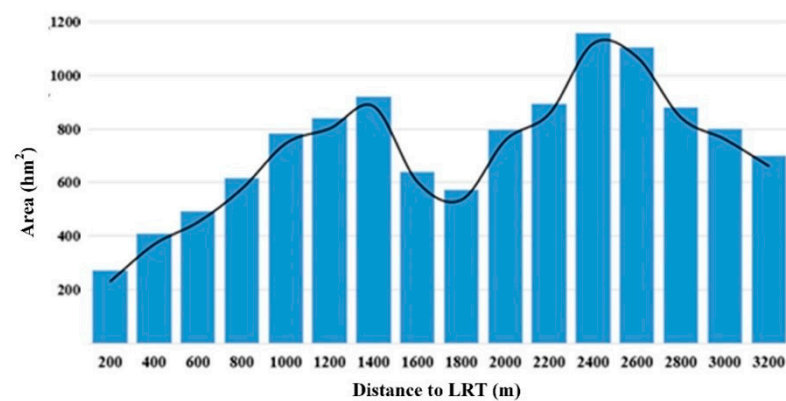

Figure 5. Absolute area change of LUC (farmland to construction) near the LRT line with various distances.

As shown in Figure 6, decay trend fitting can be described with a Gaussian curve between relative change rate K by Equitation (4) and spatial distance to the LRT line. This function provides a decline in the conversion rate of change applied by farmland for development as construction land according to its LU and distances. First, the LRT leads to considerable impacts within the first to ninth buffers (i.e., 200–1800 m), described by progressive improvement in the conversion rate of LU change with increasing distance from the LRT. A very sharp decline in K(d) could be observed as we move away from the existing areas (1.4 km~2 km) to the point where it finally drops slowly after 2 km.
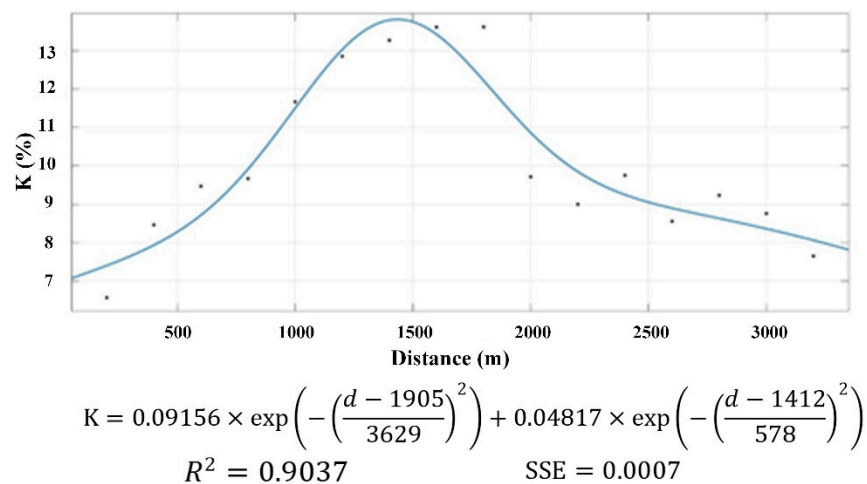
$$K = 0.09156 \times \exp\left(-\left(\frac{d - 1905}{3629}\right)^2\right) + 0.04817 \times \exp\left(-\left(\frac{d - 1412}{578}\right)^2\right)$$

$$R^2 = 0.9037 \qquad\qquad SSE = 0.0007$$

Figure 6. Fitting result between relative change rate and distance to the LRT line.

Different intraregional effects were employed to determine the LRT planning influence. The spillover means that the LRT induces spatial damping in developing LU. Thus, the LU conversion probability will be very low. The generated aggregation indicates that the LRT spatially pulls the LU development, which increases the LU conversion probability. As shown in Figure 7, five-year transition potential maps (i.e., from 2001 to 2005) were generated by the LRT impact constructed into the CA model according to Equitation (5).
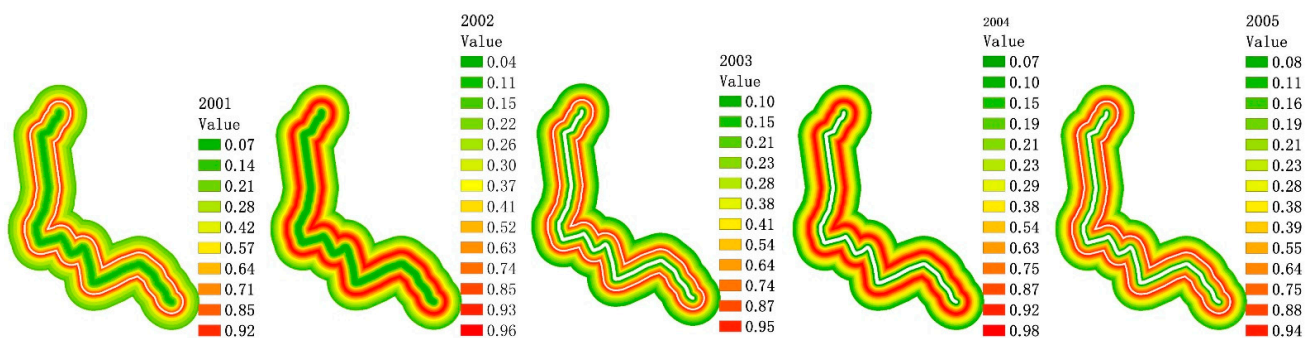

Figure 7. Transition potential maps generated by the LRT impact using the proposed method.

The final transition probability was generated by Equation (6). The transition potentials of each year and each LU type were utilized in the CA-based LUC simulation.

4.2. Model Parameter Result

4.2.1. Transition Possibility Threshold Result

Some samples were randomly selected to determine $P_{threshold}$ through a recursive procedure in the simulation of the year 2000 based on the year 1995, accomplished by comparing the actual LU pattern with the simulated results for different transition possibility threshold parameters. The determination of $P_{threshold}$ in this work can be divided into two main parts, which are rough and refined matching, according to Zhu [10]. The rough matching takes the changes in the number of grids of each land-use type as the index to determine the initial threshold range. Figure 8a shows the actual LUC cells in number and simulated LUC cells of different LU types with different $P_{threshold}$ during the year 1995 to 2000. The curves show the good result of the proposed method (i.e., the simulated value is very close to the actual one) at $P_{threshold}$ of approximately 0.25–0.35. The refined matching is further used to obtain the optimal threshold by verifying the accuracy of the model within a smaller margin. The simulation accuracy of LU-type construction is evaluated using the FoM indicator to investigate the optimal $P_{threshold}$. Figure 8b describes the relationship between $P_{threshold}$ (with a 0.02 step size in the interval [0.26, 0.36]) and the

LU change performance in 2000 through the proposed CA model. It can be seen that the maximum value of the FoM indicator was obtained for $P_{\text{threshold}} = 0.3$.
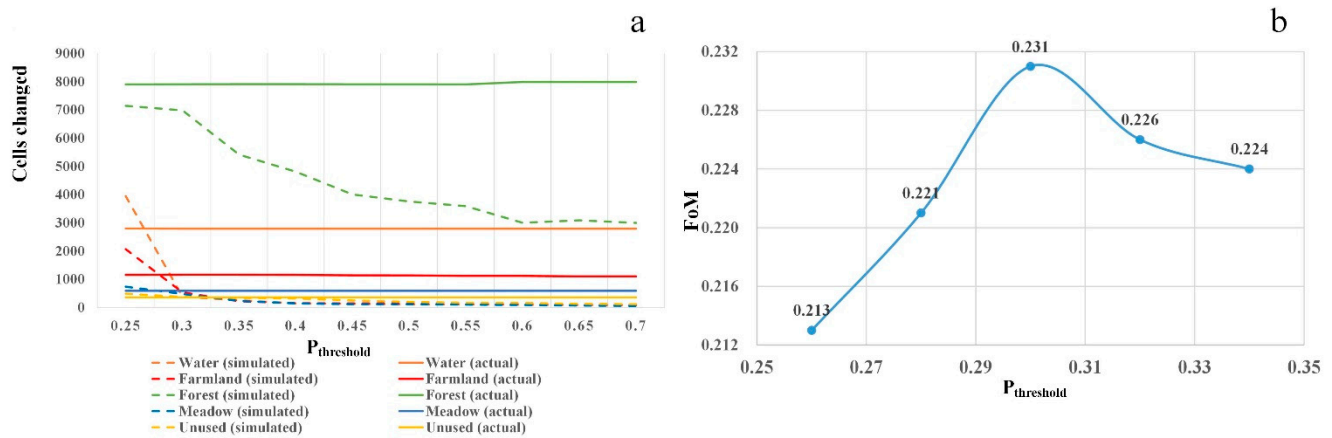

Figure 8. Model performance of different transition possibility threshold $P_{\text{threshold}}$ values. (**a**) relationship between the cell number changed (simulated vs. actual) and different $P_{\text{threshold}}$; (**b**) relationship between $P_{\text{threshold}}$ and FoM.

4.2.2. Iteration Ending Condition Result by Markov Chain

Table 3 presents the transition area matrix between the years 2000 and 2005, obtained from the Markov chain. All of the original LU types have an inheritance degree close to one. The neighborhood conditions and the mentioned transition matrices were adopted to calculate the local neighborhood probability for each cell ($N_{i \to j}$). Liu et al. showed that superior simulation results could be obtained by the iteration number of an integer multiple observation [4]. Therefore, the iteration number from 2000 to 2005 was chosen as 20, while the number of interval iterations per year was four. Thus, the LRT constraint is incorporated in the model after 24 iterations.

Table 3. Transfer matrices at Nanjing in the range 2000–2005.

	Construction	Unused	Forest	Water	Farmland	Meadow
Construction	407.94	0.15	0.59	26.26	51.32	0.12
Unused	0.68	1.33	0.28	0.00	0.00	0.02
Forest	40.23	0.02	231.09	0.11	2.01	0.03
Water	26.28	0.00	0.86	237.84	17.90	0.00
Farmland	195.82	0.09	1.48	118.55	1226.02	1.28
Meadow	0.00	0.03	2.14	1.54	0.03	20.34

Notes: Row denotes inflow: column denotes outflow, unit: km^2.

4.3. LUC Simulation Results

The proposed CA model was finally executed using $P_{\text{threshold}} = 0.30$ and the above-mentioned iteration-ending condition. The simulation was performed in discrete temporal steps. Figure 9 shows the final LU simulation result of the year 2005. Compared to the actual LU pattern in 2005 (see Figure 2c), the proposed method can simulate the spatial structure of LU well. An overall FoM is 0.231, which is acceptable.
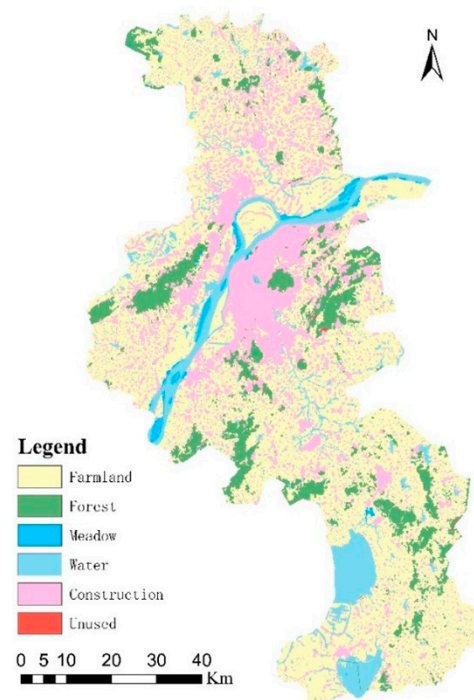
Figure 9. Simulated LU pattern in the year 2005 by the proposed CA model.

Table 4 summarizes the FoM accuracies of LU simulation for different districts. As shown in Table 4, developed areas, including Zhucheng, Qixia, and Jiangning, provided higher accuracy than underdeveloped ones, such as Gaochun, Liuhe, and Lishui, demonstrating the compatibility with the urban development level. The accuracy in forestry, meadow, and water was relatively stable because they are ecologically protected zones in the southern region. Since the unused land area is small, the simulation results are more affected by other random factors. Thus, the accuracy variance across districts is high in the unused land.

Table 4. The FoM accuracies of LU simulation in different districts by the proposed model.

| Districts /LU	Water	Farmland	Construction	Unused	Meadow	Forestry
Qixia	0.186	0.212	0.251	0.225	0.214	0.216
Pukou	0.197	0.225	0.221	0.169	0.211	0.214
Zhucheng	0.206	0.211	0.276	0.178	0.185	0.219
Jiangning	0.215	0.212	0.245	0.203	0.224	0.213
Liuhe	0.212	0.222	0.223	0.210	0.219	0.221
Lishui	0.222	0.215	0.192	0.218	0.231	0.211
Gaochun	0.216	0.214	0.208	0.221	0.216	0.221

4.4. Comparison of CA Simulation between with/without Considering LRT Influence Factor

A CA model without LRT factors (i.e., only Con_{topo}, $Con_{planning}$, and $P_{distance}$) was also constructed to prove that the CA model can achieve superior performance when considering the LRT influence. Then, the model accuracies (FoM) of different districts and LU types were calculated. As shown in Table 5, the proposed method provides a promising performance in these three districts, where the FoM value is higher than 0.24. However, compared with the existing developed regions (Zhucheng and Qixia), lower accuracy could be obtained for Jiangning as a newly developed area. This may be due to the complexity of urban development, which means that underdeveloped areas are mainly driven by urban expansion.

Table 5. Construction land validation (FoM) for various districts, simulated by the proposed and comparative methods.

	Qixia	Jiangning	Zhucheng	Pukou	Liuhe	Lishui	Gaochun
LRT impact	0.251	0.245	0.276	0.221	0.223	0.192	0.208
NO LRT	0.190	0.186	0.174	0.221	0.223	0.192	0.208

The urban land was also simulated without considering the LRT influence. According to Table 5, higher simulation accuracies could be obtained in the mentioned three districts in the presence of the LRT influence. Figure 10 compares the results qualitatively. Since LRT in Nanjing runs through the Qixia, Zhucheng, and Jiangning districts, the simulation results of these three districts will be emphasized in this study. As shown in Figure 10, the spatial structure of the patches in the simulated map by LRT is very similar to the actual growth map, as indicated by a more evident conversion of farmland to construction land (see red boxes in Figure 10).
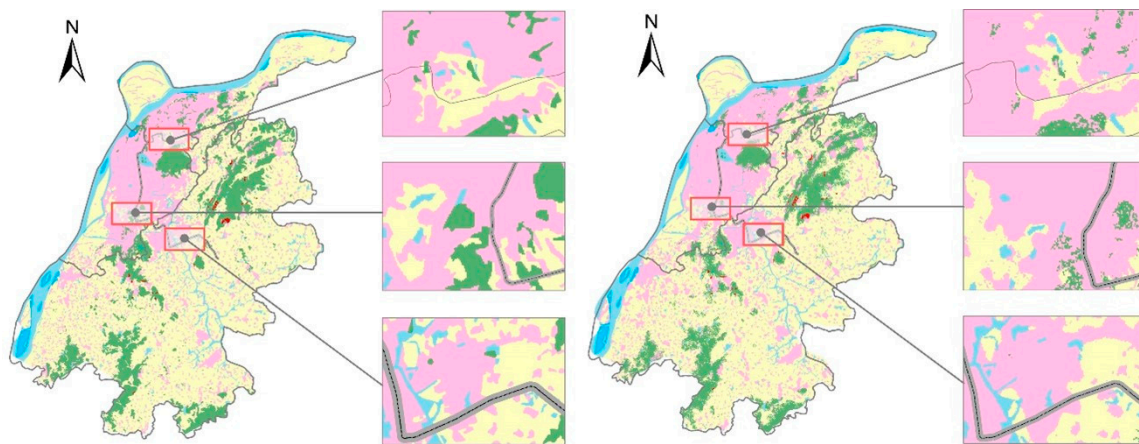
Figure 10. Comparison of the simulated results: left: without considering the LRT influence, right: LRT influence (the proposed model).

4.5. Comparison of CA Simulation between with/without Considering Spatiotemporal Heterogeneity of LRT Influence

The advantage of incorporating the spatiotemporal heterogeneity of LRT influence into the CA model is demonstrated through the LU change simulation with a comparative study with the linear relationship in space and time [40]. Figure 11 compares the simulated results of the proposed model with a linear model for different buffer zones. In a simple comparison, each farmland in each ring was converted into construction land under the force of linear mode. The relative error rates between the actual and simulated urban LU results in 2005 for different rings are shown in Table 6. It could be seen that the relative growth rate of the construction LU in most rings obtained by linear mode was excessively higher than that of the spatial structure with actual ones, as indicated by the higher relative error values. Table 6 also indicates that the proposed model can provide less accuracy than the linear model in the increasing growth rate of construction LU change within 1000 to 1400 m. The main reason for this is that the growth rate of the construction LU within this stage may be compatible with the linear growth mode, implying that the spatiotemporal heterogeneity of the LRT influence for dynamic LU change can be modeled by multiple fitting decay functions, benefiting from the similar work on the neighborhood influence of the LU change [54,56]. As a result, the results essentially indicate that the proposed model incorporated the spatiotemporal heterogeneity of the LRT influence could be utilized to simulate the heterogeneity LUC development.
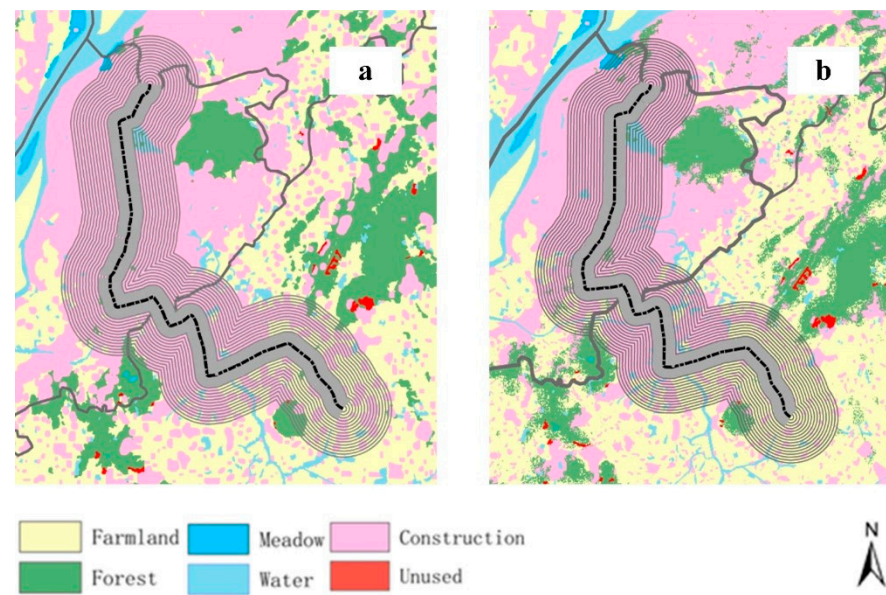
Figure 11. Detailed comparison of the simulated results near the LRT line. (**a**) Classic linear model, (**b**) the proposed model.

Table 6. The relative error rates between the actual and simulated urban LU results in 2005 for different rings.

Distance (m)	Relative Error		Distance (m)	Relative Error	
	Ours	Linear		Ours	Linear
0–200	1.74%	5.11%	1600–1800	7.69%	18.74%
200–400	1.78%	4.31%	1800–2000	5.25%	22.66%
400–600	1.23%	8.09%	2000–2200	4.67%	23.24%
600–800	0.37%	14.30%	2200–2400	3.89%	22.78%
800–1000	6.83%	12.64%	2400–2600	0.81%	26.08%
1000–1200	8.38%	7.03%	2600–2800	2.99%	21.23%
1200–1400	9.79%	6.16%	2800–3000	5.21%	11.55%
1400–1600	8.16%	11.68%	3000–3200	5.32%	10.23%

To more clearly express the information of errors in Table 6 and investigate the causes, Figure 12 (in red boxes) illustrates that the proposed model provides a slightly lower growth rate of the construction land than the actual one in the different buffer zones. Like many traditional methods [22,31,33], the LRT's effect on the LU development was verified in this study using the hypothesis that the LRT influence is the same within the same buffer. Affected by the spatial location difference, even if some LU blocks have similar distances to LRT, they obtain heterogeneous LRT influence. For example, according to studies performed by Liu et al. [57] and Todes et al. [58], the LRT in the city center has little influence on the spatial form, while the urban space expansion is most active surrounding the LRT in the urban fringe, and the land development surrounding the peripheral urban part is asymmetrical in space. Hence, even though the blocks have similar distances to LRT, the effect type (aggregation or spillover effect) and the LRT strengths on them may still be different. The study area in the next stage of this research was employed to obtain more robust results, while extending in the next stage of this research.
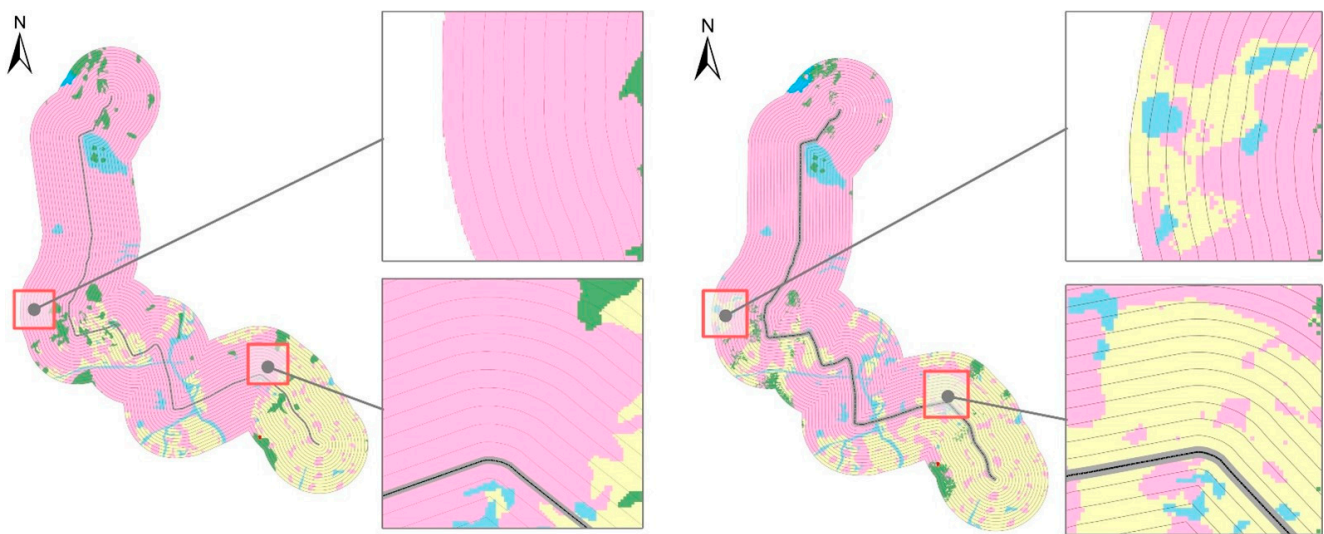
Figure 12. Comparison of the simulated results with different buffer zones in 2005: left: actual map, right: our result.

5. Conclusions

This study investigates the interactions between rail transit and LUC to capture the spatiotemporal heterogeneity of urban development and verify how their results can be translated into the effect function in CA modelling and simulation goals. In the current work, the distance decay function was utilized to investigate the impact of LRT on LUC. The main change trends of each LU type (mainly from farmland to construction land) over different stages can be explained by time and space. The cellular automata (CA) model incorporated with LRT impact was finally established and implemented for simulating the LUC in Nanjing city, China.

The fitting decay function (i.e., Gauss distribution) was utilized for analyzing the spatiotemporal heterogeneity of LRT influence. The LRT leads to considerable impacts within the 200–1800 m range. A very sharp effect decline could be observed when the distance comes to 1.4 km~2 km, and finally drops slowly after 2 km. This relationship was then considered in the CA-based LUC simulation.

The proposed method provides a promising performance with the FoM values generally higher than 0.24. A comparison between CA simulation with and without LRT influence demonstrates that the relative error rates between the actual and simulated LU pattern significantly decrease through the LRT model. FOM focuses on the change in land-use rather than the continuity of land classes. Even though its relevance in land-use modelling has been acknowledged, criticism and questions about its effectiveness persist. As the changes are rarely drastic, the FOM values are often very low (Li shui and Gao chun in Table 5), which neglects the direction of land-use transformation. Comprehensive evaluation should be calculated in measuring agreement in future work.

This study can enrich the existing study of the interactions between rail transit and LU change and provide a methodology framework to make proactive spatial planning interventions for sustainable urban development. However, the scenario of a single LRT line was considered in this study. Thus, a superior understanding of the interactions between an LRT network and LU change will be explored in future work.

Author Contributions: Conceptualization, Jie Zhu; algorithm, Jiaming Na and Jie Zhu; process the data, Jie Zhu and Shaoning Di; writing—original draft preparation Jiaming Na and Jie Zhu; writ-ing—review and editing, Jiazhu Zheng, Hu Ding and Lingfei Ma; funding acquisition, Jie Zhu and Hu Ding. All authors have read and agreed to the published version of the manuscript.

References

1. Clarke, K.C.; Hoppen, S.; Gaydos, L. A self-modifying cellular automaton model of historical urbanization in the San Francisco Bay area. *Environ. Plan. B Plan. Des.* **1997**, *24*, 247–261. [CrossRef]
2. Verburg, P.H.; de Nijs, T.C.; van Eck, J.R.; Visser, H.; de Jong, K. A method to analyse neighbourhood characteristics of land use patterns. *Comput. Environ. Urban Syst.* **2004**, *28*, 667–690. [CrossRef]
3. Seto, K.C.; Fragkias, M.; Güneralp, B.; Reilly, M.K. A meta-analysis of global urban land expansion. *PLoS ONE* **2011**, *6*, e23777. [CrossRef] [PubMed]
4. Liu, X.; Liang, X.; Li, X.; Xu, X.; Ou, J.; Chen, Y.; Li, S.; Wang, S.; Pei, F. A future land use simulation model (FLUS) for simulating multiple land use scenarios by coupling human and natural effects. *Landsc. Urban Plan.* **2017**, *168*, 94–116. [CrossRef]
5. Wu, F. Calibration of stochastic cellular automata: The application to rural-urban land conversions. *Int. J. Geogr. Inf. Sci.* **2002**, *16*, 795–818. [CrossRef]
6. Pontius, R.G.; Boersma, W.; Castella, J.-C.; Clarke, K.; de Nijs, T.; Dietzel, C.; Duan, Z.; Fotsing, E.; Goldstein, N.; Kok, K. Comparing the input, output, and validation maps for several models of land change. *Ann. Reg. Sci.* **2008**, *42*, 11–37. [CrossRef]
7. Liu, Y. Modelling sustainable urban growth in a rapidly urbanising region using a fuzzy-constrained cellular automata approach. *Int. J. Geogr. Inf. Sci.* **2012**, *26*, 151–167. [CrossRef]
8. Rafiee, R.; Mahiny, A.S.; Khorasani, N.; Darvishsefat, A.A.; Danekar, A. Simulating urban growth in Mashad City, Iran through the SLEUTH model (UGM). *Cities* **2009**, *26*, 19–26. [CrossRef]
9. Feng, Y. Modeling dynamic urban land-use change with geographical cellular automata and generalized pattern search-optimized rules. *Int. J. Geogr. Inf. Sci.* **2017**, *31*, 1198–1219. [CrossRef]
10. Zhu, J.; Sun, Y.; Song, S.; Yang, J.; Ding, H. Cellular automata for simulating land-use change with a constrained irregular space representation: A case study in Nanjing city, China. *Environ. Plan. B Urban Anal. City Sci.* **2020**. [CrossRef]
11. National Bureau of Statistics of China. *Communiqué of the National Bureau of Statistics of People's Republic of China on Major Figures of the 2010 Population Census*; National Bureau of Statistics of China: Beijing, China, 2011.
12. Cervero, R.; Dai, D. BRT TOD: Leveraging transit oriented development with bus rapid transit investments. *Transp. Policy* **2014**, *36*, 127–138. [CrossRef]
13. Yang, P.; Wei, C. Metro-city planning practice: Wuhan example (in Chinese). *Planners* **2016**, *32*, 5–10.
14. Wang, X.-F.; Xu, J.-G.; Li, Y.-F. Potential influences of rail transportation construction to land use differentiation in Nanjing. *Hum. Geogr* **2005**, *20*, 112–116.
15. Zhang, M.; Wang, L. The impacts of mass transit on land development in China: The case of Beijing. *Res. Transp. Econ.* **2013**, *40*, 124–133. [CrossRef]
16. Thapa, R.B.; Murayama, Y. Drivers of urban growth in the Kathmandu valley, Nepal: Examining the efficacy of the analytic hierarchy process. *Appl. Geogr.* **2010**, *30*, 70–83. [CrossRef]
17. Duranton, G.; Turner, M.A. Urban growth and transportation. *Rev. Econ. Stud.* **2012**, *79*, 1407–1440. [CrossRef]
18. Joshi, H.; Guhathakurta, S.; Konjevod, G.; Crittenden, J.; Li, K. Simulating the effect of light rail on urban growth in Phoenix: An application of the UrbanSim modeling environment. *J. Urban Technol.* **2006**, *13*, 91–111. [CrossRef]
19. Pacheco-Raguz, J.F. Assessing the impacts of Light Rail Transit on urban land in Manila. *J. Transp. Land Use* **2010**, *3*, 113–138. [CrossRef]
20. Bardaka, E.; Delgado, M.S.; Florax, R.J. Causal identification of transit-induced gentrification and spatial spillover effects: The case of the Denver light rail. *J. Transp. Geogr.* **2018**, *71*, 15–31. [CrossRef]
21. Wang, J.; Feng, Y.; Ye, Z.; Tong, X.; Wang, R.; Gao, C.; Chen, S.; Lei, Z.; Liu, S.; Jin, Y. Simulating the effect of urban light rail transit on urban development by coupling cellular automata and conjugate gradients. *Geocarto Int.* **2020**, 1–19. [CrossRef]
22. Ratner, K.A.; Goetz, A.R. The reshaping of land use and urban form in Denver through transit-oriented development. *Cities* **2013**, *30*, 31–46. [CrossRef]
23. Calvo, F.; de Oña, J.; Arán, F. Impact of the Madrid subway on population settlement and land use. *Land Use Policy* **2013**, *31*, 627–639. [CrossRef]
24. Mokadi, E.; Mitsova, D.; Wang, X. Projecting the impacts of a proposed streetcar system on the urban core land redevelopment: The case of Cincinnati, Ohio. *Cities* **2013**, *35*, 136–146. [CrossRef]
25. Comber, S.; Arribas-Bel, D. "Waiting on the train": The anticipatory (causal) effects of Crossrail in Ealing. *J. Transp. Geogr.* **2017**, *64*, 13–22. [CrossRef]

26. Pan, H.; Zhang, M. Rail transit impacts on land use: Evidence from Shanghai, China. *Transp. Res. Rec.* **2008**, *2048*, 16–25. [CrossRef]
27. Bhattacharjee, S.; Goetz, A.R. The rail transit system and land use change in the Denver metro region. *J. Transp. Geogr.* **2016**, *54*, 440–450. [CrossRef]
28. Ahmad, S.; Avtar, R.; Sethi, M.; Surjan, A. Delhi's land cover change in post transit era. *Cities* **2016**, *50*, 111–118. [CrossRef]
29. Iacono, M.J.; Levinson, D.M. Predicting land use change: How much does transportation matter? *Transp. Res. Rec.* **2009**, *2119*, 130–136. [CrossRef]
30. Hurst, N.B.; West, S.E. Public transit and urban redevelopment: The effect of light rail transit on land use in Minneapolis, Minnesota. *Reg. Sci. Urban Econ.* **2014**, *46*, 57–72. [CrossRef]
31. Golub, A.; Guhathakurta, S.; Sollapuram, B. Spatial and temporal capitalization effects of light rail in Phoenix: From conception, planning, and construction to operation. *J. Plan. Educ. Res.* **2012**, *32*, 415–429. [CrossRef]
32. Cervero, R. Linking urban transport and land use in developing countries. *J. Transp. Land Use* **2013**, *6*, 7–24. [CrossRef]
33. Tan, Z.; Li, S.; Li, X.; Liu, X.; Chen, Y.; Li, W. Spatio-temporal effects of urban rail transit on complex land-use change. *Acta Geogr. Sinica* **2017**, *72*, 850–862.
34. Li, S.; Liu, X.; Li, Z.; Wu, Z.; Yan, Z.; Chen, Y.; Gao, F. Spatial and temporal dynamics of urban expansion along the Guangzhou–Foshan inter-city rail transit corridor, China. *Sustainability* **2018**, *10*, 593. [CrossRef]
35. Zhang, H.; Li, X.; Liu, X.; Chen, Y.; Ou, J.; Niu, N.; Jin, Y.; Shi, H. Will the Development of a High-Speed Railway Have Impacts on Land Use Patterns in China? *Ann. Am. Assoc. Geogr.* **2019**, *109*, 979–1005. [CrossRef]
36. Rodriguez, D.A.; Vergel-Tovar, E.; Camargo, W.F. Land development impacts of BRT in a sample of stops in Quito and Bogotá. *Transp. Policy* **2016**, *51*, 4–14. [CrossRef]
37. Aljoufie, M.; Brussel, M.; Zuidgeest, M.; van Delden, H.; van Maarseveen, M. Integrated analysis of land-use and transport policy interventions. *Transp. Plan. Technol.* **2016**, *39*, 329–357. [CrossRef]
38. Lin, J.; Chen, T.; Han, Q. Simulating and predicting the impacts of light rail transit systems on urban land use by using cellular automata: A case study of Dongguan, China. *Sustainability* **2018**, *10*, 1293. [CrossRef]
39. Zhao, L.; Shen, L. The impacts of rail transit on future urban land use development: A case study in Wuhan, China. *Transp. Policy* **2019**, *81*, 396–405. [CrossRef]
40. Yang, J.; Shi, F.; Sun, Y.; Zhu, J. A cellular automata model constrained by spatiotemporal heterogeneity of the urban development strategy for simulating land-use change: A case study in Nanjing City, China. *Sustainability* **2019**, *11*, 4012. [CrossRef]
41. Li, X.; Yang, Q.; Liu, X. Discovering and evaluating urban signatures for simulating compact development using cellular automata. *Landsc. Urban Plan.* **2008**, *86*, 177–186. [CrossRef]
42. Li, X.; Lin, J.; Chen, Y.; Liu, X.; Ai, B. Calibrating cellular automata based on landscape metrics by using genetic algorithms. *Int. J. Geogr. Inf. Sci.* **2013**, *27*, 594–613. [CrossRef]
43. Ayazli, I.E.; Kilic, F.; Lauf, S.; Demir, H.; Kleinschmit, B. Simulating urban growth driven by transportation networks: A case study of the Istanbul third bridge. *Land Use Policy* **2015**, *49*, 332–340. [CrossRef]
44. Willigers, J.; Van Wee, B. High-speed rail and office location choices. A stated choice experiment for the Netherlands. *J. Transp. Geogr.* **2011**, *19*, 745–754. [CrossRef]
45. Murakami, J.; Cervero, R. *High-Speed Rail and Economic Development: Business Agglomerations and Policy Implications*; University of California Transportation Center: Berkeley, CA, USA, 2012.
46. Garmendia, M.; Romero, V.; Ureña, J.M.D.; Coronado, J.M.; Vickerman, R. High-speed rail opportunities around metropolitan regions: Madrid and London. *J. Infrastruct. Syst.* **2012**, *18*, 305–313. [CrossRef]
47. Cao, M.; Bennett, S.J.; Shen, Q.; Xu, R. A bat-inspired approach to define transition rules for a cellular automaton model used to simulate urban expansion. *Int. J. Geogr. Inf. Sci.* **2016**, *30*, 1961–1979. [CrossRef]
48. Luo, J.; Wei, Y.D. Modeling spatial variations of urban growth patterns in Chinese cities: The case of Nanjing. *Landsc. Urban Plan.* **2009**, *91*, 51–64. [CrossRef]
49. Shu, B.; Bakker, M.M.; Zhang, H.; Li, Y.; Qin, W.; Carsjens, G.J. Modeling urban expansion by using variable weights logistic cellular automata: A case study of Nanjing, China. *Int. J. Geogr. Inf. Sci.* **2017**, *31*, 1314–1333. [CrossRef]
50. Omrani, H.; Tayyebi, A.; Pijanowski, B. Integrating the multi-label land-use concept and cellular automata with the artificial neural network-based land transformation model: An integrated ML-CA-LTM modeling framework. *GIScience Remote Sens.* **2017**, *54*, 283–304. [CrossRef]
51. Guerra, E.; Cervero, R.; Tischler, D. Half-mile circle: Does it best represent transit station catchments? *Transp. Res. Rec.* **2012**, *2276*, 101–109. [CrossRef]
52. Cao, X.J.; Porter-Nelson, D. Real estate development in anticipation of the Green Line light rail transit in St. Paul. *Transp. Policy* **2016**, *51*, 24–32. [CrossRef]
53. Kwoka, G.J.; Boschmann, E.E.; Goetz, A.R. The impact of transit station areas on the travel behaviors of workers in Denver, Colorado. *Transp. Res. Part A Policy Pract.* **2015**, *80*, 277–287. [CrossRef]
54. Barreira-González, P.; Gómez-Delgado, M.; Aguilera-Benavente, F. From raster to vector cellular automata models: A new approach to simulate urban growth with the help of graph theory. *Comput. Environ. Urban Syst.* **2015**, *54*, 119–131. [CrossRef]
55. Wu, H.; Zhou, L.; Chi, X.; Li, Y.; Sun, Y. Quantifying and analyzing neighborhood configuration characteristics to cellular automata for land use simulation considering data source error. *Earth Sci. Inform.* **2012**, *5*, 77–86. [CrossRef]

56. Feng, Y.; Tong, X. Incorporation of spatial heterogeneity-weighted neighborhood into cellular automata for dynamic urban growth simulation. *GIScience Remote Sens.* **2019**, *56*, 1024–1045. [CrossRef]
57. Jing, L. Research on the Urban Land-Use along the High-Capacity Rail Rapid Transit Line—A Case Study of Wuhan No. 2 Rail Transit Line. Ph.D. Thesis, Huazhong University of Science of Technology, Wuhan, China, 2005.
58. Todes, A. Urban growth and strategic spatial planning in Johannesburg, South Africa. *Cities* **2012**, *29*, 158–165. [CrossRef]